Analyst

CRITICAL REVIEW

View Article Online
View Journal | View Issue

Cite this: *Analyst*, 2025, **150**, 5124

An overview of utilising photo-tunable thiophene scaffolds as luminogens for chemical and biological sensing: progress and prospects

Aakash Venkatesan, Anila Rose Cherian and Aatika Nizam *

Received 21st September 2025,
Accepted 14th October 2025

DOI: 10.1039/d5an01012h

rsc.li/analyst

Thiophene, a heterocyclic compound, is widely used in various biological and chemical fields owing to its unique nature and versatile properties. Therefore, integrating thiophene rings into organic compounds has introduced a new class of structural diversification that can be effectively utilised in biological and environmental applications. As these rings bring about structural diversification in organic compounds, they are highly utilised in the synthesis of organic luminogens. The incorporation of thiophene rings into organic luminogens has gained prominence due to their versatility as electron donors, recognition units, and fluorophores. The versatility of thiophene rings provided a strategy to overcome the traditional drawbacks of ICT and PET mechanisms in the field of fluorescent sensors. Hence, this review article presents various thiophene-based fluorescent probes that address the traditional drawbacks of ICT and PET mechanisms. Through versatile strategies for incorporating thiophene rings into luminogens, these probes exhibit high sensitivity and selectivity towards biological and chemical analytes.

1. Introduction

In today's world, selective analysis *via* quantitative and qualitative aspects of chemical and biological analytes has become essential to ensure an accurate, reliable, and comprehensive understanding of substances and processes.[1] Over the centuries, various methods have been explored to estimate these analytes, which include colorimetry,[2] electrochemical,[3] high-performance liquid chromatography (HPLC),[4] flow injection spectrophotometry,[5] chemiluminescence,[6] and capillary zone electrophoresis.[7] However, the sensitivity, specificity, and

Department of Chemistry, Christ University, Bangalore, India.
E-mail: aatika.nizam@christuniversity.in

Aakash Venkatesan

Aakash Venkatesan holds a B.Sc. degree in Chemistry, Botany and Zoology from CHRIST (Deemed to be University), Bangalore, Karnataka. He is currently pursuing his M.Sc. in Chemistry at the same institution under the supervision of Dr Aatika Nizam. His work primarily focuses on the synthesis and characterisation of dual-state emissive, excited-state intramolecular proton transfer (DSE-ESIPT)-based organic luminogens, exploring their potential in therapeutic applications, alongside the development of nanocatalysts for facilitating organic transformation reactions.

Anila Rose Cherian

Dr Anila Rose Cherian received her PhD in electrochemical sensing, focusing on advanced sensor development. Her research work focuses on the development of low-cost and convenient sensors, including those used in clinical and medical diagnostics, environmental and health monitoring, and food industries; electro-organic synthesis; the voltammetric detection of food additives, pollutants, and biomolecules; the development of molecularly imprinted polymer-based sensors for the selective detection of food, additives, and biomolecules; and the synthesis of 2D materials, polymer nanocomposites, and composites of metal nanoparticles using electrochemical or chemical methods.

selectivity of sensors to detect analytes have proven to be a significant challenge in analysing them precisely.[8] Fluorescence is emitted when illuminated with a UV light source of a specific wavelength.[9] This phenomenon has drawn the attention of many researchers whose aim is to develop a sensor for the selective detection of analytes. Under physiological conditions, this method has prevailed in its significance due to its high selectivity and sensitivity,[10] facile visualization,[11] real-time detection,[12] rapid response rate,[13] and inexpensiveness.[14] To understand the phenomenon of fluorescence, various photophysical mechanisms have been put forth by researchers, which include Excited State Intermolecular Proton Transfer (ESIPT),[15] Intramolecular Charge Transfer (ICT),[16] Photoinduced Electron Transfer (PET),[17] Aggregation Caused Quenching (ACQ),[18] Aggregation Induced Enhancement (AIE),[19] and Förster Resonance Energy Transfer (FRET).[20]

Over the decades, these mechanisms have been employed to harness a wide range of organic fluorescent molecules. Among these, ICT and PET are two mechanisms that have specific disadvantages of low sensitivity and poor selectivity.[21] Consequently, it became essential to modify the ICT- and PET-based molecules for enhanced selectivity towards analytes. These mechanism-based probes predominantly contain an electron-donating group, which plays a pivotal role in the selective recognition of analytes by enhancing or quenching fluorescence.[16,17] Thus, many modifications have been made by substituting various electron-donating moieties, such as diethylamino,[22] triphenylamine,[23] pyrrolidine,[24] and ethoxy groups.[25] Even though they are highly electron-rich donating groups, they protonate under acidic conditions and lose their electron-donating capacity, which limits their functionality under acidic conditions.[26] Thus, the requirement for an alternative electron-rich donating moiety is that it functionalizes as a recognition group and does not protonate under acidic conditions. In the search for such electron-donating moieties, the attention of researchers has been drawn towards heterocyclic compounds that contain sulfur atoms (thiophene). These compounds exhibit a higher electron density than other heterocyclic compounds (furan or pyrrole) that can adsorb selective ions onto the surface.[27] Due to their ease of synthetic alterations and environmental stability, thiophene derivatives demonstrate a high level of structural diversification, combined with the potent polarizability of the sulfur atom in the ring, which imparts stability to the conjugated system, resulting in enormous electrical and charge-transfer capabilities.[28,29] They also exhibit thermal, optoelectronic, and photoluminescence properties, such as high photophysical tunability, good charge mobility, the ability to promote a lower band gap, and a high adsorption coefficient.[30,31] However, its utility in emissive applications is hindered by its restricted fluorescence quantum yield in both solution and solid states, which can be attributed to the heavy sulfur atom present in the ring and rigid packing in the solid state, causing a quenching effect.[32,33] Regardless of its limitations, the multifaceted properties forecast thiophene rings as π conjugate linkers, electron-rich donors, and recognition groups.[30] In the past few years, the employment of heterocyclic thiophene rings in fluorescent probes has gained significant attention, and various approaches have been put forth to elevate the fluorescence efficiency and widen the application of thiophene-based fluorescent probes.[34] In this review, we flaunt various constructions of thiophene-based fluorescent probes that overcame their limitations over the years (2020–24) and proved their versatility in incorporating thiophene rings as π linkers, electron-donating moieties, and fluorophores for the selective and efficient determination of various chemical and biological analytes.

Aatika Nizam

Dr Aatika Nizam received her M. Sc. degree in Chemistry from Bangalore University, Karnataka, India, in 2006. She finished her Ph.D. degree in Chemistry from Bangalore University, Karnataka, India, in 2012. Currently, she is an Associate Professor in the Department of Chemistry at CHRIST (Deemed to be University), Bangalore, India. Her research interests include organic synthesis, heterocyclic chemistry, synthesis of nano-catalysts and their application in organic transformation reactions, photoluminescence studies, and spectroscopy.

2. Mechanism of thiophene-based probes

2.1. Intramolecular charge transfer (ICT)

π-System structure with electron accepting and electron donating groups at the ends is referred to as push–pull molecules, which exhibit an intramolecular charge-transfer (ICT) process that contributes to the fluorescence emission.[35] Due to the ICT process, the excited state exhibits a relatively higher polarization and dipole moment than the ground state.[34] Therefore, the construction of ICT-based fluorescent probes comprises a fluorophore, electron acceptor base (A), and electron donor base (D), conjugated by a π linker structure, and is depicted as a D–π–A system, as shown in Fig. 1. The recognition group in the ICT-based probes and the interaction of analytes with D or A groups determine whether the spectrum is a bathochromic or hypsochromic shift.[36] Brevus reported the importance of participating components in the D–π–A system, which had

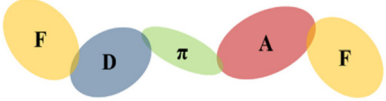

Fig. 1 Visual depiction of the ICT-based synthetic approach.

structural effects on the ICT process.[37] Therefore, thiophene, with a versatile ring structure, good charge mobility, and high photophysical properties, is extensively utilized as a D group and a π conjugate linker in ICT-based fluorescent probes for the selective recognition of analytes.[29,30]

2.1.1. Thiophene as an electron-donating group. Chao *et al.* demonstrated Probe 1 (Fig. 2) based on the ICT mechanism, which comprises pyrene as a fluorophore as well as an acceptor base, thiophene as the donor base, and α, β-unsaturated ketone as a π linker. This D–π–A system assisted in the emission of yellow fluorescence *via* charge transfer from pyrene to thiophene. Introducing an analyte that binds to the π bridge hinders charge transfer in the system, leading to the emission of blue fluorescence by the pyrene moiety. A hypsochromic shift is also observed because of the hindered charge transfer in the system.[38] Probe 2 (Fig. 2) was proposed by Bhuvanesh *et al.* utilizing an ICT mechanism possessing an ester group as the acceptor base and thiophene as the donor base, forming a D–π–A system. No fluorescence emission was observed upon the charge transfer in the system. Upon adding the analyte, the system coordinated with the analyte, making the acceptor and donor weak, which restricted the charge transfer that initiated the red fluorescence emission in the probe. Based on this analysis, the turn-on fluorescence emission is observed in probe.[39] An ICT-based fluorescent Probe 3 (Fig. 2) was developed by Purushothaman *et al.* with conjugated thiophene as the fluorophore, thiophene ring as the donor base, and benzothiazole as the acceptor base as well as receptor. This construction exhibited a bright green fluorescence emission through charge transfer from thiophene to benzothiazole. The analyte binds to the N atoms of benzothiazole and the π-linker, which restricts efficient charge transfer in the system, leading to a bathochromic shift in the emission spectra from green to yellow in the solution state and from green to red in the solid state.[40]

2.1.2. Thiophene as π conjugate linker. Zhao *et al.* synthesized Probe 4 (Fig. 2) in accordance with the ICT mechanism, possessing benzothiazole as the fluorophore, triphenyl amine as the strong donor base, cyanide group as a strong acceptor base, and thiophene as the π conjugate linker through which the charge transfer occurs, and initiated the blue fluorescence of benzothiazole. Upon the interaction of the analyte with the acceptor base, it becomes a highly accepting group that actively promotes efficient charge transfer and facilitates the red fluorescence of benzothiazole. A red shift is also observed due to the binding of the analyte with the acceptor base.[41] Chemchem *et al.* proposed Probe 5 (Fig. 2) based on the ICT mechanism, which comprises coumarin as the fluorophore, hydroxyl group as a weak donor base, cyanide group as a strong acceptor base, and thiophene ring as the π bridge linker. Due to the presence of a weak donor base, charge transfer is hindered, resulting in no fluorescence emission. Upon introducing an analyte that can deprotonate the hydroxyl protons on the probe, it converts it from a weak donor base to a strong donor base, aiding the charge transfer from the donor to the recipient. This, in turn, activated the coumarin fluorophore in the probe, providing green fluorescence in the presence of the analyte, and a hypsochromic shift was also noticed due to the interaction with the electron-donating moiety.[42] Razi *et al.* elucidated Probe 6 (Fig. 2) with respect to the ICT mechanism, which contains benzothiazole as the fluorophore as well as the acceptor base, imidazole as the donor base, and thiophene as the π bridge linker. Cyan blue fluorescence emission is observed due to the protruding charge transfer from imidazole to benzothiazole. Upon adding the analyte, it coordinates with the N and S atoms of the π linker in the probe, which prevents the donor and acceptor moiety charges from transferring to one another. Depending on the nature of the analyte and the strength of the coordination, there may be quenching or shifts in the emission spectrum.[43]

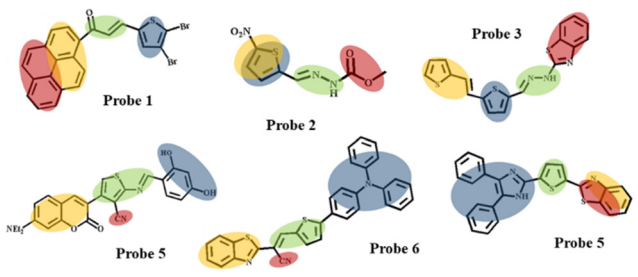

Fig. 2 Structural diversity of ICT-based thiophene probes developed using different synthetic strategies.

2.2. Photoinduced electron transfer (PET)

The construction of a PET-based system comprises a recognition group (R) and an electron-donating moiety attached to a fluorophore (F) through a spacer (S), as depicted in Fig. 3.[44] There are two ways in which this mechanism works: either on–off or off-on fluorescence emission. When illuminated with radiation, electron transfer from the donor moiety to the fluorophore is observed, which limits the emission intensity of the fluorophore. When an object binds to the recognition site of the system, photo-induced electron transfer is restricted, which turns on the emissive nature of the fluorophore.[45] However, upon binding transition metals to the recognition site, the redox behavior of the 3d orbital electron metal center facilitates electron transfer either from the metal to the fluorophore or *vice versa*, which quenches the emissive nature of the fluorophore.[46] The utilization of the recognition moiety and donor moiety, collectively called the receptor in the system, determines the fate of the fluorescence response. Therefore, thiophene, being an electron-rich donor moiety, a high reco-

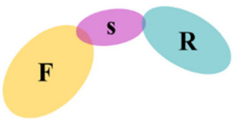

Fig. 3 Visual depiction of the PET-based synthetic approach.

gnition group, and possessing high photophysical tunability, has been broadly utilized in PET-based systems for the specificity and selectivity sensing of various analytes.[29,30]

Xing *et al.* synthesized fluorescent Probe 7 (Fig. 4) with a thiophene substituent as the fluorophore and the diethylaminophenol groups as the donor bases, with recognition groups present in it. As this construction contains two donor moieties that transfer electrons to the fluorophore, it gives rise to a strong PET response that quenches the fluorescence. Upon adding the analyte to the probe, the recognition groups in the structure coordinate with the analyte and hinder electron transfer across the system, which assists the emissive nature of the fluorophore in emitting a strong yellow fluorescence.[47] Sarkar *et al.* proposed Probe 8 (Fig. 4), which contains thiophene as a donor base as well as a recognition group and pyrene as a fluorophore. The donor base transfers electrons to the fluorophore, enhancing the PET response towards the system, which leads to fluorescence quenching. Upon disrupting the donor base *via* protonation or coordination with the analyte, charge transfer is restricted in the system, leading to an enhanced fluorescence response by the fluorophore by emitting strong blue fluorescence.[48] Karakuş *et al.* developed fluorescent Probe 9 (Fig. 4), which comprises thiophene as the recognition site, as well as donor base and anthracene as the fluorophore. Due to electron transfer between the thiophene and anthracene rings, fluorescence emission is not observed. Upon allowing the probe to coordinate with an analyte, coordination takes place with the sulphur atoms of the thiophene, restricting electron transfer throughout the probe. Hence, this restricted charge transfer enhances the fluorescence intensity and emits green fluorescence.[49]

Xing *et al.* elucidated Probe 10 (Fig. 4) by possessing a phenolic substituent as a weak donor base as well as a recognition group and thiophene as the fluorophore. The charge transfer in the system from the donor moiety to the fluorophore led to fluorescence quenching. Upon subjecting the probe to a certain analyte, the recognition group of the phenolic substituent is bound to it and makes the system rigid, which restricts charge transfer and contributes to the enhanced fluorescence response by emitting bright green fluorescence. Additionally, the presence of the ethylenedioxy moiety on the fluorophore enhances the fluorescence intensity.[50] Yin *et al.* developed fluorescent Probe 11 (Fig. 4) with salicylic aldehyde substituent as recognition site as well as electron donor, and thiophene as the fluorophore moiety. The donor base transfers electrons to the fluorophore, which limits the fluorescence emission. Upon introducing the analyte to the probe, it binds to the recognition sites of the salicylic aldehyde substituent and hinders electron transfer in the probe, which enhances the fluorescence emission intensity, thus emitting strong blue fluorescence by the probe.[51] Kolcu *et al.* proposed fluorescent Probe 12 (Fig. 4), which incorporated triphenylamine as the fluorophore and thiophene as the recognition as well as donor base. Thiophene transfers electrons to triphenylamine, restricting the fluorescence response. In the presence of a specific analyte, the S and N atoms of the sensor bind to the analyte, which inhibits electron transfer in the system. This inhibition allows the sensor to emit strong blue fluorescence.[52]

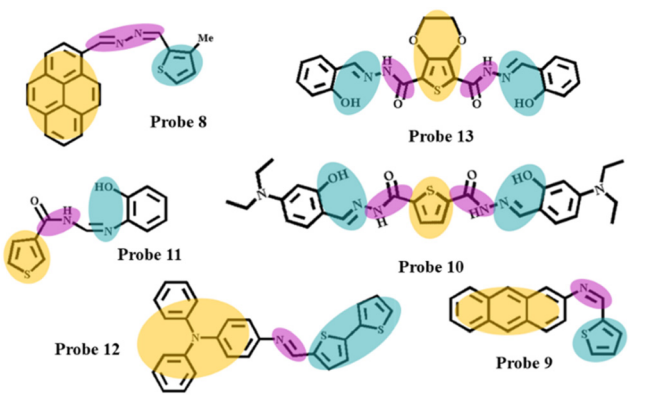

Fig. 4 Structural diversity of PET-based thiophene probes developed using different synthetic strategies.

3. Strategies for the synthesis of thiophene-based probes

The synthesis of thiophene-based fluorescent probes is established by incorporating various thiophene derivatives into the systems as per the requirements of the probe. Thiophene, being a versatile heterocyclic ring, has multifaceted properties as a fluorophore,[47,51] electron donor base,[38,40] π conjugate linker,[41,43] and recognition moiety.[48,49] Thiophene is incorporated by various reactions, including acylation,[53] Schiff's base condensation,[54] Claisen–Schmidt,[55] Suzuki–Miyaura coupling,[56] Knoevenagel condensation,[41] and Wittig reactions.[57] Despite multiple reactions put forth by researchers to incorporate thiophene into the probe, derivatives of thiophene-carboxaldehyde and thiophene-carbohydrazide (Fig. 5b) are most commonly used as precursors for this purpose because they possess an active aldehyde and amine group that can be incorporated in various reactions.[58] Therefore, in this particular section of the review, we introduced various synthesis methods of thiophene-based fluorescent probes with derivatives of thiophene-carboxaldehyde and thiophene-carbohydrazide as their precursors.

3.1. Thiophene-carboxaldehyde as a precursor

Li *et al.* synthesized fluorescent Probe 13 (Fig. 6) involving 5-methyl-thiophene-carboxaldehyde and rhodamine hydrazide. The reaction involved condensation of an aldehyde group in

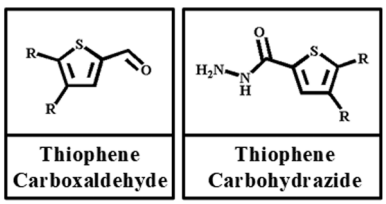

Fig. 5 Major precursors for thiophene-based probes.

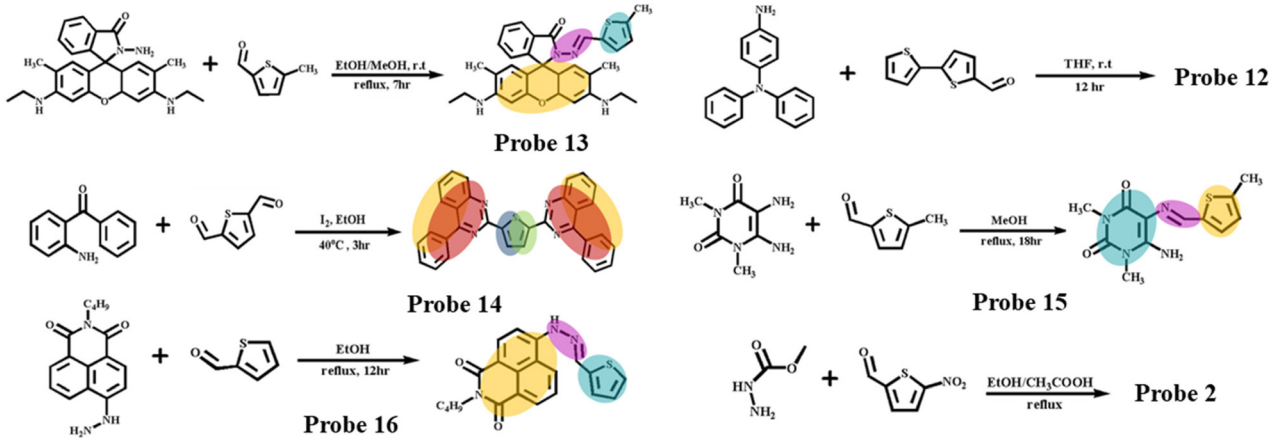

Fig. 6 Synthetic routes involving thiophene-carbohydrazide as precursors for thiophene-based probes.

5-methyl-thiophene-carboxaldehyde and an amino group in rhodamine hydrazide in methanol/ethanol (1 : 1, v/v) solution and refluxed for 7 h at room temperature. It yields a yellow precipitate wherein thiophene acts as a donor as well as a recognition unit and rhodamine as a fluorophore in the system, and the probe was then characterized using ^{1}H NMR.[54] Kolcu *et al.* utilized 2,2′-bithiophene-5-carboxaldehyde with 4-amino-triphenylamine to prepare fluorescent Probe 12 (Fig. 6) by forming an imine group through the condensation of an aldehyde and the amino group of the precursor in THF, followed by stirring at room temperature for 12 h; here, bithiophene behaves as a recognition unit and triphenylamine as a fluorophore in the system. The presence of a dark yellow precipitate confirmed the formation of the product, and it was characterized using ^{1}H NMR, ^{13}C NMR, and FTIR.[52] Fluorescent Probe 14 (Fig. 6) was designed by Harsha *et al.* with a reaction mixture of ethanol containing thiophene-2,5-dicarbaldehyde, aminobenzophenone, and ammonium acetate in the presence of iodine as the catalyst, which was stirred at 40 °C for 3 h. The resultant crude was purified, yielding a golden yellow powder. This reaction brought out a phenyl quinazoline group in the system, which acted as a fluorophore as well as an acceptor base and thiophene as a donor base. The probe was then characterized using ^{1}HNMR, ^{13}CNMR, ESI-MS, and ESI-HRMS analyses.[59] Hammud *et al.* employed a condensation reaction between methyl-2-thiophene-carboxaldehyde, 5,6-diamino-1,3-dimethyluracil hydrate, and p-toluene sulfonic acid in a methanol medium, which was refluxed for 18 h at room temperature to form Schiff base Probe 15 (Fig. 6). Upon recrystallization, a solid orange precipitate was obtained, in which uracil units behaved as a recognition group and thiophene acted as a fluorophore in the system. The obtained precipitate was characterized using ^{1}H NMR and FTIR.[60] Fluorescent Probe 16 (Fig. 6) was prepared by Saini *et al.* using 2-butyl-6-hydrazino-benzo isoquinoline-1,3-dione as the initial constituent in an ethanol medium along with thiophene-2-carbaldehyde, which was refluxed at room temperature for 12 h. Upon recrystallization of crude in acetonitrile, an orange solid precipitate was obtained, in which the quinoline derivative acted as a fluorophore and thiophene acted as a recognition site, and it was characterized using ^{1}H NMR, ^{13}C NMR and ESI-MS.[61] Bhuvanesh *et al.* prepared fluorescent Probe 2 (Fig. 6) by a simple condensation reaction between 5-nitro-2-thiophenecarboxaldehyde and methyl carbazate in the presence of acetic acid in an ethanolic medium and obtained a greenish yellow precipitate. Upon recrystallization of the crude extract, yellow crystals were formed in which the ester moiety acted as the acceptor base and thiophene behaved as the donor base, forming a D–π–A system, and it was characterized using ^{1}H NMR, ^{13}C NMR, and ESI-MS.[39] By complying with all the synthetic strategies, the use of thiophene-carboxaldehyde as a precursor for developing thiophene-based probes is illustrated in Fig. 6.

3.2. Thiophene-carbohydrazide as a precursor

Kundu *et al.* utilized thiophene-2-carbohydrazide along with pyrene-1-carbaldehyde to synthesize fluorescence Probe 17 (Fig. 7) by condensing the aldehyde group of pyrene-1-carbaldehyde and the amino group of thiophene-2-carbohydrazide in methanol and refluxed for 8 h at 70 °C, which formed a Schiff's base where thiophene acted as a donor group and pyrene acted as an acceptor as well as a fluorophore moiety in the system. Deep-yellow single crystals indicated the formation of the probe and were characterized by ^{1}HNMR, FTIR, HRMS, and X-ray crystallography.[62] Mathew *et al.* synthesized fluorescent Probe 18 (Fig. 7) by a straightforward condensation reaction between 2-hydroxynaphthaldehyde and thiophene-2,5-dicarbohydrazide in an ethanolic medium containing acetic acid, which was refluxed for 6 h at room temperature. The dark yellow precipitate observed indicates the formation of a Schiff's base, which contains thiophene as a fluorophore and a hydroxyl group as a recognition site. It was characterized using ^{1}H NMR, ^{13}C NMR, and FTIR.[63] Yin *et al.* prepared fluorescent Probe 11 (Fig. 7) by condensing thiophene-3-carbohydrazide with salicylaldehyde in an ethanolic medium and refluxing for 4 h at room temperature. The formation of the Schiff's base was indicated by the precipitation of a white solid product in which thiophene acted as a fluorophore and

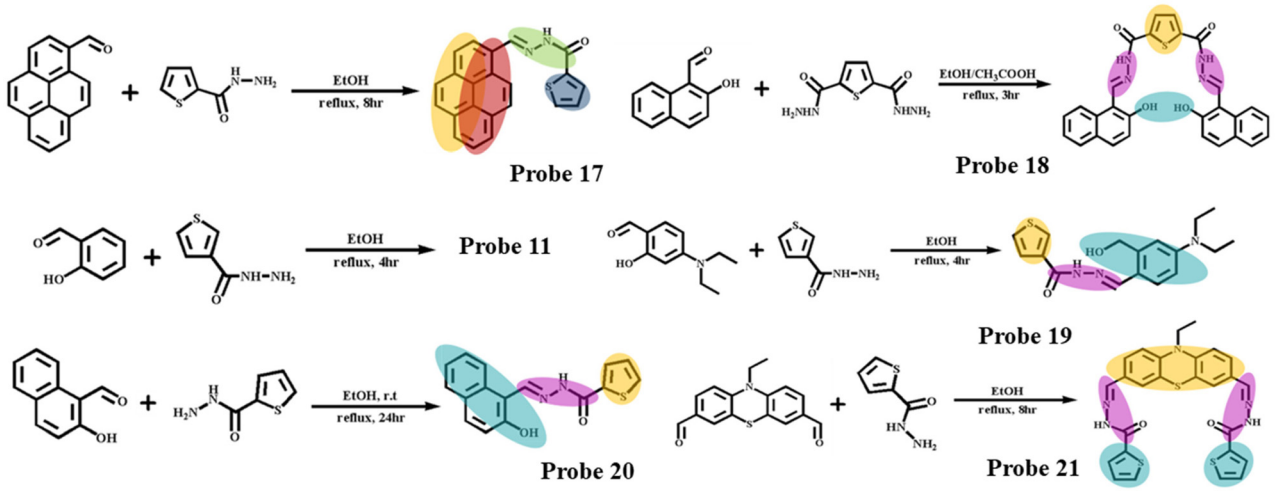

Fig. 7 Synthetic routes involving thiophene-carbohydrazide as precursors for thiophene-based probes.

hydroxyl groups acted as recognition units in the probe. The synthesized probe was characterized by ^{1}H NMR, ^{13}C NMR, and FTIR.[51] Li *et al.* demonstrated the synthesis of fluorescent Probe 19 (Fig. 7) by the condensation of the aldehyde group in 4(*N*,*N*-diethylamino) salicylaldehyde and the amino group in thiophene-3-carbohydrazide in dry ethanol and refluxed for 4 h at room temperature. The formation of a yellow solid indicated the presence of a product where hydroxyl groups acted as recognition sites and thiophene acted as a fluorophore in the system, and the probe was characterized by ^{1}H NMR and FTIR.[64] Fluorescent Probe 20 (Fig. 7) was designed by Tiwari *et al.* by a condensation reaction between 2-hydroxy-1-naphthaldehyde and thiophene-2-carbohydrazide in an ethanolic medium and refluxed at room temperature for 24 h, which contained thiophene as a fluorophore and hydroxyl group as a recognition site in the system. Upon recrystallization, pale yellow crystals were obtained, which were characterized by FTIR, ^{1}H NMR, ^{13}C NMR, and ESI-MS.[65] Govindasamy *et al.* synthesized fluorescent Probe 21 (Fig. 7) by condensing 10-ethyl-10H-phenothiazine-3,7-dicarbaldehyde with thiophene-2-carbohydrazide in ethanol medium under reflux for 8 h at room temperature, leading to the formation of a Schiff base compound. The product obtained is a yellow precipitate, where phenothiazine behaves as a fluorophore and thiophene acts as a recognition unit in the system, and it is characterized by FTIR, ^{1}HNMR, and ^{13}CNMR.[66] By complying with all the synthetic strategies, the use of thiophene-carbohydrazide as a precursor for developing thiophene-based probes is illustrated in Fig. 7.

4. Applications of thiophene-based probes

Advanced thiophene-based luminogens, along with their photophysical changes towards chemical and biological analytes, are illustrated in Table 1.

4.1. Sensing cations

Complying with all thiophene-based probes used for sensing cations is illustrated in Fig. 8 and 9.

4.1.1. Aluminium ions. A new thiophene-salicylic aldehyde Schiff base fluorescence Probe 11 was demonstrated by Yin *et al.* for the fluorometric analysis of aluminum ions in both solid and solution states. The probe did not display any considerable fluorescence emission due to the electron transfer in the system that quenched the fluorophore, but the intensity increased, and a new peak at 463 nm was observed due to the increment in the concentration of aluminum ions. This was ascribed to the chelation effect of aluminum ions with the probe that restricted the electron transfer in the system, providing a bright turn-on blue emission spectrum, and the detection limit was estimated to be 49 nM.[51] A rhodamine-thiophene-based fluorescent Probe 13 was developed by Li *et al.*, which was utilized for the selective detection of aluminum ions in an aqueous medium. Upon excitation at 530 nm, weak emission intensity was observed at 588 nm in DMF, which was due to the inhibition of the fluorophore expression by electron transfer in the system. Upon introducing aluminum ions, an enhanced emission intensity peak at 588 nm was observed. This is ascribed to the chelation effect, which restricts the electron transfer in a system that unblocks the fluorophore to exhibit yellow fluorescence emission. The detection limit was found to be 4.17 μM.[54] A new thiophene-based turn-on fluorescent Probe 19 was synthesized by Li *et al.* for the selective recognition of aluminum ions in the solution state. When the probe was excited at 375 nm, no significant fluorescence emission was observed. However, the addition of aluminum ions generated a new emission peak at 475 nm with bright blue fluorescence. This was attributed to the chelation-enhanced fluorescence effect that hindered electron transfer across the system, which enhanced fluorescent emission. The detection limit was found to be 0.3 nM.[64] Tiwari *et al.* prepared a thiophene-naphthaldehyde-based fluorescent Probe 20 for the sen-

Table 1 Structures of thiophene-based probes and their photophysical changes

Sensing ions	Probe	Probe structures	Photo physical change	Limit of detection (LOD)	Ref.
Cu ions	40	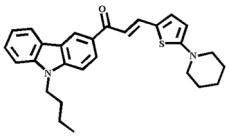	Green fluorescence to turn-off fluorescence	0.29 μM	82
	41	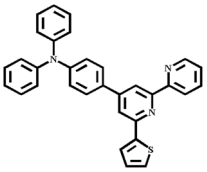	Green fluorescence to turn-off fluorescence	0.789 μM	83
Cd ions	42	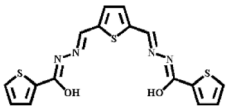	Yellow fluorescence to red fluorescence	88.96 nM	84
	43	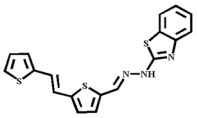	Green fluorescence to yellow fluorescence	0.1 μM	40
Hg ions	44	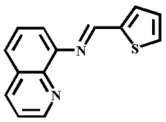	Cyan blue fluorescence to turn-off fluorescence	23.4 nM	85
	45	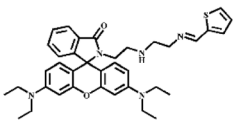	Turn off fluorescence to yellow fluorescence	0.19 μM	86
	46	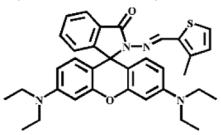	Turn off fluorescence to orange fluorescence	7.5 μM	87
	47	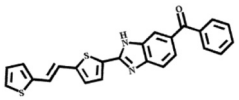	Cyan blue fluorescence to turn-off fluorescence	0.06 nM	88
	48	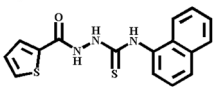	Turn-off fluorescence to blue fluorescence	4.92 μM	89
	49	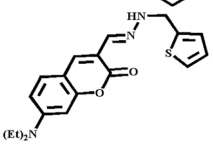	Blue fluorescence to turn-off fluorescence	5.15 nM	90
	50	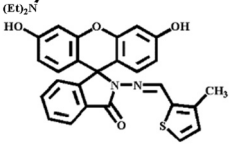	Turn-off fluorescence to lime green fluorescence	137 nM	91
Fe ions	51	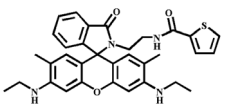	Turn off fluorescence to yellow fluorescence	5 μM	53
	52	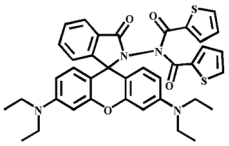	Turn off fluorescence to red fluorescence	3.76 μM	92

Table 1 *(Contd.)*

Sensing ions	Probe	Probe structures	Photo physical change	Limit of detection (LOD)	Ref.
Ni ions	53	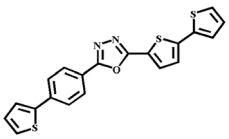	Turn off fluorescence to blue fluorescence	3 μM	93
ClO ions	54	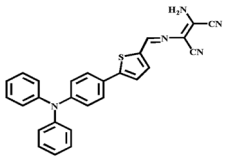	Turn off fluorescence to blue fluorescence	—	94
	55	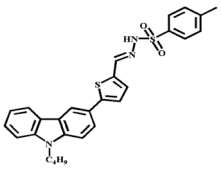	Blue fluorescence to yellow fluorescence	1.16 μM	95
NH_2NH_2	56	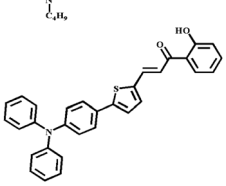	Red fluorescence to blue fluorescence	0.23 μM	96
H_2O_2	58	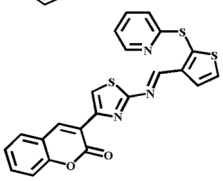	Turn off fluorescence to green fluorescence	0.15 μM	97

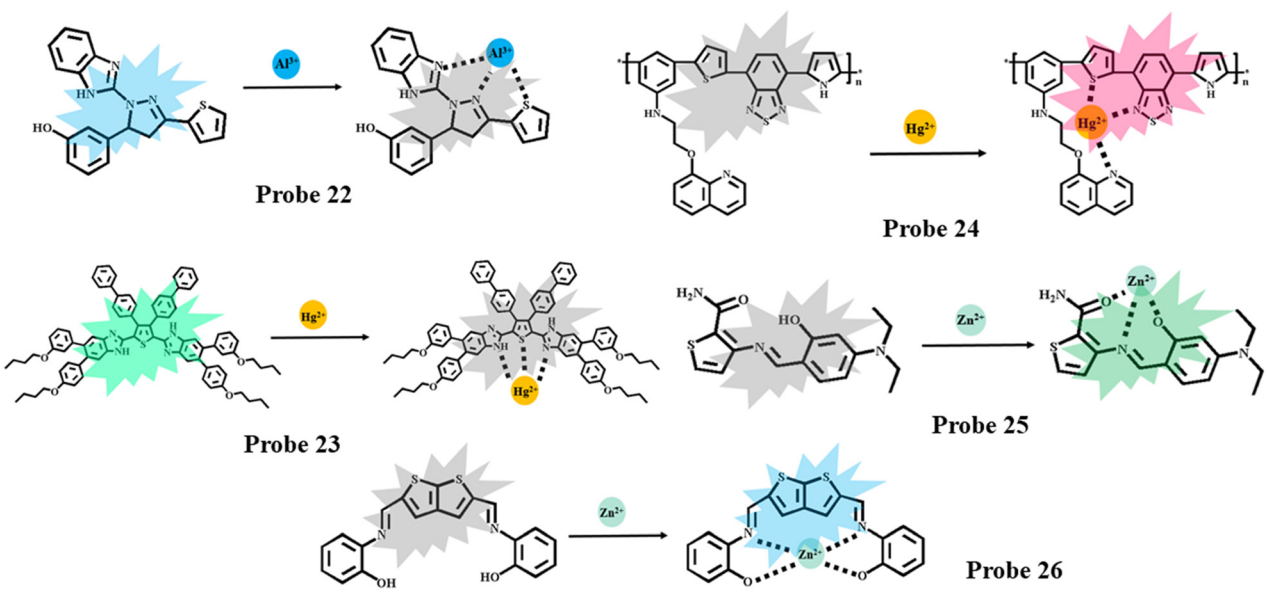

Fig. 8 Thiophene-based Probes 22–26 depicting structural transformations upon selective sensing of metal cations, including Al^{3+}, Hg^{2+}, and Zn^{2+}.

sitive and selective identification of aluminum ions in an aqueous medium. Upon excitation at 407 nm, the probe exhibited a weak emission intensity with a dual peak, which was shouldered at 476 and 452 nm. Upon introducing aluminum ions, the emission peaks, which were shouldered at 476 and 452 nm, started to enhance and provided a bright blue

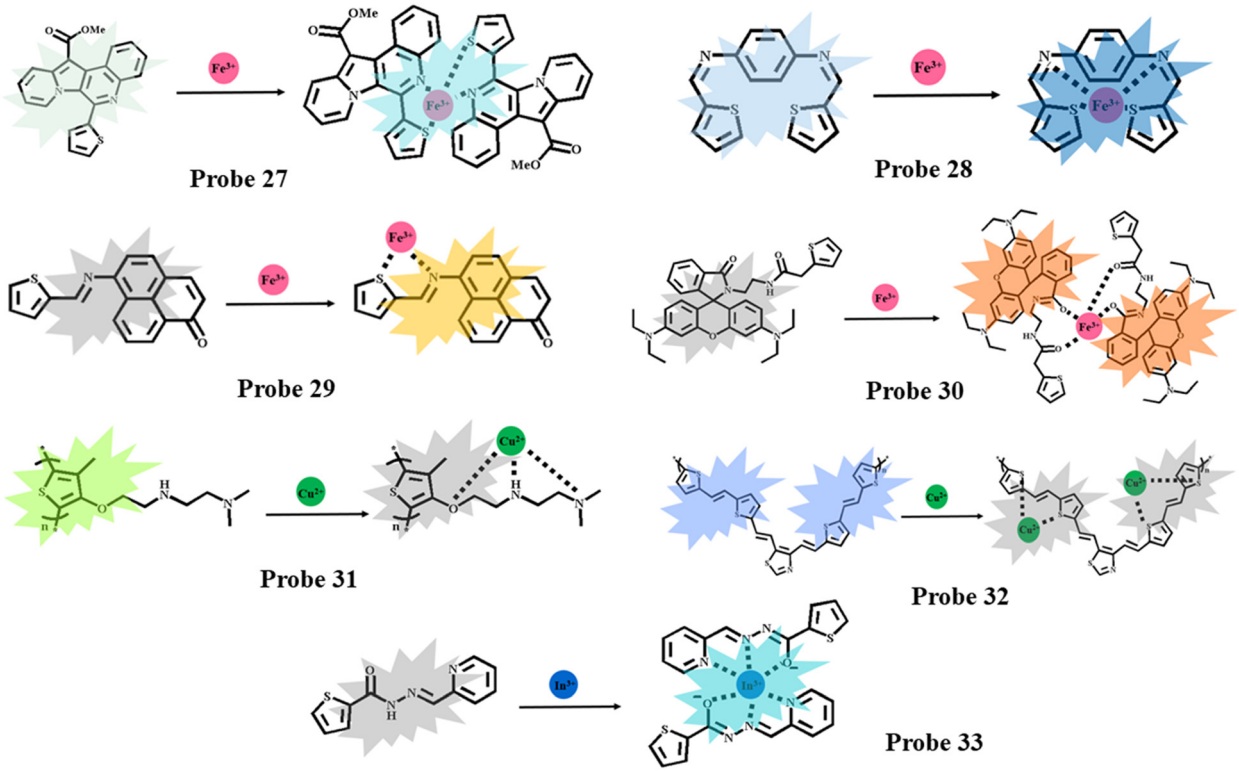

Fig. 9 Thiophene-based Probes 27–33 illustrating structural changes upon selective sensing of metal cations, including Fe^{3+}, Cu^{2+}, and In^{3+}.

fluorescence emission. This was ascribed to the restricted intramolecular charge transfer on the complexation of the probe with aluminum, and the detection limit was estimated to be 1.35 nM.[65] M. Rangasamy and K. Palaninathan synthesized thiophene-integrated pyrazoline-based fluorescent Probe 22 (Fig. 8) for selective recognition of aluminum ions. The probe exhibits a bright blue fluorescence emission peak at 447 nm. Upon the addition of aluminum ions, the emission peak at 447 nm starts to reduce along with quenching of fluorescence emission. This was due to the chelation-caused quenching that restricted the intramolecular charge transfer in the system on complexation with aluminum ions, leading to quenching of the fluorescent emission, and the limit of detection was estimated to be 89.2 nM.[55]

4.1.2. Mercury ions. Thiophene-imidazole-derived fluorescent Probe 6 was proposed by Razi *et al.* for the ratiometric detection of mercury ions in both solid and solution states. Upon excitation at 395 nm, the emission peak was shouldered at 513 nm, exhibiting cyan blue fluorescence. A hypsochromic shift of about 28 nm was noticed upon the addition of mercury ions to the aqueous medium, and a new peak was observed at 495 nm, exhibiting a strong blue fluorescence emission. This shift was ascribed to the chelation effect that contributed to the variation in the charge transfer in the D–π–A system, and the limit of detection was revealed to be 28 nM.[43] A thiophene-pyrene-based fluorescent Probe 8 was synthesized by Sarkar *et al.*, which was utilized for the identification of mercury ions in an aqueous medium. There was no significant fluorescence emission at 452 nm upon excitation at 355 nm. Upon the addition of mercury ions, a bathochromic shift of about 15 nm was recorded with an increase in emission intensity, providing a strong blue emission spectrum. This was ascribed to the complexation of mercury ions with the probe, which disturbed the electron transfer and the π–π stacking of the pyrene unit during complexation. Therefore, the detection limit was evaluated to be 30.6 nM.[48] A phenothiazine-thiophene-based fluorescent Probe 21 was developed by Govindasamy *et al.* for the analysis of mercury ions in the solution state. Upon excitation at 422 nm, the probe exhibited lime green fluorescence emission with a shoulder peak at 537 nm. Upon introducing mercury ions, the emission intensity peak at 537 nm started to quench and was completely quenched upon introducing 1.2 eq. of mercury ions. This was ascribed to the charge transfer in the system on complexation with mercury ions, which quenched the fluorescent intensity, and the limit of detection was found to be 4.4 nM.[66] Thiophene-bis(benzimidazole)-based fluorescent Probe 23 (Fig. 8) was synthesized by A. Kumar and P. S. Chae for trace estimation of mercury ions in the solution state. Upon excitation at 400 nm, the probe displayed bright cyan blue fluorescent emission with a peak shouldered at 488 nm. Upon introducing mercury ions, the emission peak at 488 nm starts to quench and the emission intensity also quenches completely with 2 eq. of mercury ions. This was ascribed to the chelation-caused quenching that restricted the electron/charge transfer in the system, leading to quenching of the fluorescent

emission, and the detection limit was evaluated to be 0.047 pM.[67] Feng *et al.* synthesized polymer fluorescent Probe 24 (Fig. 8) containing thiophene, benzothiazole, and quinoline groups, which were used for the selective recognition of mercury ions in an aqueous medium. No significant fluorescent emission was observed in the probe. Upon introducing mercury ions, enhanced red fluorescent emission was observed. This was due to the complexation of mercury with the probe, which restricted the electron transfer in the system that activated the fluorophore of the system to provide enhanced fluorescence emission, and the limit of detection was found to be 3.6 μM.[68]

4.1.3. Zinc ions. Novel thiophene-diocarbohydrazide-based Schiff's base fluorescent Probe 18 was developed by Mathew *et al.*, which was utilized for sensing zinc in an aqueous medium. The probe displayed a weak fluorescence emission upon excitation at 420 nm. However, on complexation with zinc ions, a sharp increment in the fluorescence emission from light green to bright green was observed. This was attributed to the chelation-enhanced fluorescent effect, which hindered electron transfer across the system, leading to enhanced fluorescent emission. The detection limit was estimated to be 0.15 μM.[63] Novel thiophene-based luminogenic Probe 25 (Fig. 8) was prepared by Kim *et al.* for the selective analysis of zinc ions in an aqueous medium. Upon excitation at 446 nm, the probe revealed a feeble green fluorescence emission peak at 508 nm. Upon the addition of zinc ions, there was a significant increase in the emission intensity peak at 508 nm. This was ascribed to the restricted proton transfer in the system by the complexation of zinc ions with the probe, which led to the chelation-enhanced fluorescence of the probe. The detection limit was found to be 2.55 μM.[69] Musib *et al.* synthesized new thiophene-based aggregation-induced fluorescence Probe 26 (Fig. 8) for the selective recognition of zinc ions in the solution state. Weak blue emission was noticed in the probe with a fluorescence peak at 428 nm. Upon introducing zinc ions, there was a red shift of about 27 nm, and enhanced fluorescence intensity was observed with a new peak shouldered at 455 nm. This significant enhancement was ascribed to the chelation of zinc with the probe, which restricted the electron transfer in the system, and the limit of detection was estimated to be 52.6 μM.[70]

4.1.4. Ferric ions. Harsha *et al.* synthesized novel thiophene-phenylquinazoline-derived fluorescent Probe 14 for the ratiometric detection of ferric ions in an aqueous medium. Upon excitation at 362 nm, the probe exhibited a bright blue fluorescence intensity at 427 nm. Upon introducing ferric ions to the probe solution, a red shift was noticed, and an unusual peak shouldered at 533 nm, providing a strong yellow fluorescence emission. This was ascribed to the intramolecular charge transfer in the probe by chelation of ferric ions to the probe, which created a charge transfer between the ions and system, leading to a bathochromic shift of about 106 nm, and the detection limit and quantification were found to be 20 nM and 61 nM.[59] A novel thiophene-based fluorescent Probe 27 (Fig. 9) was synthesized by Lim *et al.* for the selective recognition of ferric ions in the solution state. Upon excitation at 417 nm, the probe revealed a feeble green fluorescence emission, but upon addition of ferric ions to the solution, a dual peak with bright blue fluorescence emission was observed. This was attributed to the complexation of the ferric ions with the probe, which hindered the electron transfer in the system to enhance the fluorescence emission of the probe, and the limit of detection was estimated to be 5.2 nM in ethanol and 1.0 μM in water.[71] Berhanu *et al.* synthesized novel thiophene-based fluorescent Probe 28 (Fig. 9f) for sensing ferric ions. Upon excitation at 365 nm, the probe revealed a feeble fluorescence with an emission peak at 440 nm. Upon the addition of ferric ions, the emission peak at 440 nm started to increase, and enhanced blue fluorescence emission was recorded. This was due to the chelation of the ferric ions with the probe that restricted the electron transfer in the system, leading to an enhanced fluorescence response, and the detection limit was evaluated to be 0.38 μM.[72] Novel thiophene-phenalenone-based fluorescent Probe 29 (Fig. 9g) was developed by M Üçüncü for the detection of ferric ions in an aqueous medium. The probe showed a feeble fluorescence emission at 590 nm in acetonitrile. Upon introducing ferric ions into the probe solution, enhanced fluorescence emission was observed due to cleavage of the C=N bond in the probe that made the fluorophore exist freely in the solution, leading to enhanced fluorescence emission, and the detection limit was found to be 1.3 μM.[73] Wang *et al.* synthesized thiophene-rhodamine-based fluorescent Probe 30 (Fig. 9h) for the sensitive detection of ferric ions in a solution state. The probe showed a weak fluorescence emission with an emission peak at 584 nm when excited at 530 nm. Upon introducing the ferric ions, a significant fluorescent response was recorded due to the chelation of ferric ions with the probe that initiated the structural change, which activated the fluorescence emission response of the fluorophore, and the limit of detection was found to be less than 0.1 μM.[74]

4.1.5. Chromium ions. A new anthracene-thiophene turn-on fluorescent Probe 9 was prepared by E. Karakuş for the identification of chromium ions in aqueous and solid media. When excited at 366 nm, the probe did not display any notable fluorescence emission. This was attributed to the photo-induced electron transfer in the system, which contributed to the quenching of the fluorescence emission. However, upon introducing chromium ions, a significant cyan blue fluorescence emission was noticed. This was ascribed to the hydrolysis of the C=N bond in the probe that inhibited the electron transfer in the system, which led to an emergency fluorescence intensity peak at 500 nm and the detection limit was estimated to be 0.4 μM.[49] A new thiophene-triphenylamine derived Schiff base fluorescence Probe 12 was prepared by Kolcu *et al.* for the selective recognition of chromium ions in aqueous medium. The probe displayed a feeble fluorescence emission in THF/H_2O (v : v, 1 : 1), which shouldered at 501 nm, due to the transfer of electrons on the system. Upon adding chromium ions to the probe, a hypsochromic shift was noticed, and the emission peak was shouldered at 471 mm with enhanced blue fluo-

rescence emission. This can be ascribed to the chelation of chromium ions to the probe, which restricts electron transfer throughout the system, providing enhanced fluorescence emission, and the limit of detection was evaluated to be 1.5 μM.[52]

4.1.6. Copper ions. Novel benzothiazole-thiophene-based fluorescent Probe 6 was synthesized by Razi *et al.* for the identification of copper ions in both solution and solid state. The probe exhibited cyan blue fluorescence upon excitation at 395 nm. Upon the addition of copper ions, the emission peak at 513 nm reduced, and fluorescence intensity quenched. This can be ascribed to the chelation effect, hindering charge transfer across the system, which quenched the emission intensity of the probe. The detection limit was estimated to be 7.5 nM.[43] New diaminouracil-thiophene-based fluorescent Probe 15 was prepared by Hammud *et al.* for the analysis of copper ions in the solution state. Upon excitation at 341 nm, the probe exhibited a significant emission intensity peak shouldered at 385 nm. Upon introducing copper ions, the fluorescence intensity at 385 nm decreased, and the fluorescence emission quenched. This was ascribed to the chelation of the copper ions with the probe, which hindered proton transfer in the system, leading to fluorescence quenching. The limit of detection and quantification were found to be 0.088 μM and 0.267 μM, respectively.[60] Guo *et al.* synthesized thiophene-based polymer fluorescent Probe 31 (Fig. 9) for the detection of copper. The probe exhibited a bright green fluorescent emission in a THF/Tris–HCl mixture when excited at 412 nm. Upon introducing copper ions, the emission peak, which is shouldered at around 525 nm, starts to quench with a reduction in the fluorescence emission. This was ascribed to the chelation-caused quenching that hindered the electron/charge transfer in the system, leading to quenches of the fluorescent emission, and the detection limit was estimated to be 2.52 nM.[75] A new thiophene-thiazole-based polymer Probe 32 (Fig. 9) was prepared by K. Mahesh and S. Karpagam for the recognition of copper ions in aqueous medium. The probe exhibited a blue emission peak around 440 nm, but upon introducing copper ions, the peak, which was shouldered at 440 nm, started to diminish and was completely quenched in the presence of 4 eq. of copper ions. This is due to the complexation of copper ions with the probe. This complexation hindered the electron transfer in the system, which led to fluorescence quenching, and the detection limit was estimated to be 10.4 μM.[57]

4.1.7. Indium and gallium ions. A salicylic aldehyde-thiophene-based luminogenic Probe 7 was designed by Xing *et al.* for the identification of indium ions in an aqueous medium. The probe exhibited no fluorescence emission on excitation at 380 nm, but on introducing indium ions, a peak was observed at 550 nm, which exhibited enhanced yellow fluorescence emission. The chelation of the indium ion with the probe blocked the electron transfer in the system, thereby enabling the fluorophore to exhibit enhanced fluorescence, and the limit of detection was estimated to be 44.8 nM.[47] Cho *et al.* synthesized thiophene-based fluorescent Probe 33 (Fig. 9) for the recognition of indium ions in an aqueous medium. Upon excitation at 397 nm, the probe did not exhibit any significant fluorescent emission due to the electron transfer in the system. Upon introducing indium ions, their complexation with the probe hindered the electron transfer in the system, which enhanced the blue fluorescent emission with a peak shouldering at 460 nm, and the limit of detection was estimated to be 0.61 μM.[76] Xing *et al.* synthesized thiophene-based symmetrical Schiff's base fluorescent Probe 10 for the estimation of gallium ion in the solution medium. When excited at 421 nm, no significant fluorescence emission was observed in the probe due to the electron transfer in the system, which hindered the fluorescence emission. Upon the addition of gallium ions, complexation of these ions with a probe occurred, which hindered the electron transfer in the probe, leading to enhanced green fluorescence emission with a peak shouldered at 513 nm. The epoxy in the thiophene ring contributed to the selective recognition of gallium ions, and the limit of detection was estimated to be 3.97 nM.[50]

4.1.8. Silver ions. Hammud *et al.* prepared new diaminouracil-thiophene-based fluorescent Probe 15 for the detection of silver ions in the solution state. When excited at 341 nm, the probe exhibited a significant fluorescence emission, with an intensity peak shouldered at 385 nm. Upon the addition of silver ions, the fluorescence intensity at 385 nm decreased, and the fluorescence emission quenched. This was ascribed to the chelation of the silver ions with the probe, which hindered proton transfer in the system, leading to fluorescence quenching. The limit of detection and quantification were found to be 0.088 μM and 0.267 μM, respectively.[60] A turn-on fluorescent Probe 2 was synthesized by Bhuvanesh *et al.* for the selective recognition of silver ions in the solution state. No significant emission peak was observed on excitation at 370 nm in MeOH–H_2O solution. Upon introducing silver ions, enhanced fluorescence emission was observed, with a peak shouldered around 410 nm. This was attributed to the chelation of silver ions with the probe, which hindered the intramolecular charge transfer in the system, leading to enhanced fluorescent emission, and the limit of detection was estimated to be 0.12 μM.[39]

4.2. Sensing anions

Complying with all thiophene-based probes used for sensing anions is illustrated in Fig. 10.

4.2.1. Cyanide ions. A coumarin-thiophene-derived fluorescence Probe, 5, was designed by Chemchem *et al.* for the detection of cyanide ions in an aqueous medium. No significant fluorescence intensity was observed in the probe; however, upon the addition of cyanide ions, notable increases in emission intensity were observed, transitioning from light yellow to strong green emission. ^{1}H NMR studies were performed, which revealed the deprotonation of the hydroxy group on the phenyl part, which converted the probe into a D–π–A system, leading to a strong ICT process that enhanced the fluorescence intensity, which provided a green emission. The limit of detection and quantification were found to be 0.32 μM and 1.08 μM, respectively.[42] Triphenylamine-thiophene descended fluorescent Probe 4 was synthesized by Zhao

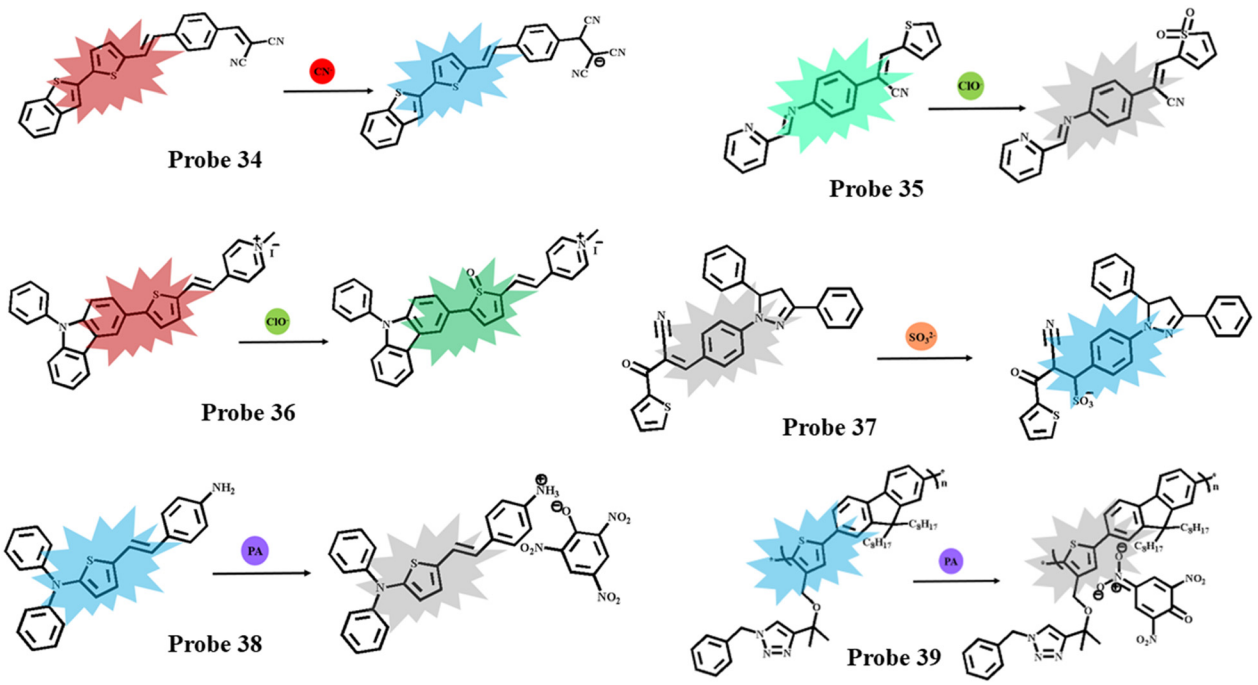

Fig. 10 Thiophene-based Probes 34–39 showing structural changes upon selective sensing of various ions, including CN^-, ClO^-, SO_3^{2-}, and picric acid (PA).

et al. and utilized for the identification of cyanide ions in the solution state. Feeble blue fluorescence emission was noticed at 565 nm when the probe was excited at 450 nm. Upon introducing cyanide ions, there was a considerable increase in the emission intensity at 545 nm. This can be attributed to the attack of cyanide ions in the cyano vinyl group of the probe, which hindered the charge transfer in the D–π–A system, leading to enhanced red fluorescence emission. This phenomenon was confirmed by performing ^{1}H NMR, and the detection limit was found to be 48.4 nM.[41] Kim *et al.* developed thiophene-derived fluorescent Probe 25 for the selective recognition of cyanide ions. When excited at 459 nm, the probe revealed a feeble green fluorescence emission peak at 528 nm, but upon introducing cyanide ions to the probe, a noticeable enhancement in fluorescence was recorded. This was ascribed to the deprotonation of the probe upon introducing cyanide ions, which suppressed the intramolecular charge transfer in the probe that enhanced the fluorescence emission, and the detection limit was estimated to be 44.6 μM.[69] Ratiometric thiophene-based fluorescence Probe 34 (Fig. 10) was designed by Popczyk *et al.* for the recognition of cyanide ions in both the solution and solid states. The probe displayed bright reddish fluorescence with an emission peak shoulder at 572 nm. Upon adding cyanide ions, the emission peak at 572 nm was reduced, and a new peak at 465 nm was observed with bright blue fluorescence. This was attributed to the interaction of the cyanide group with the probe, which disrupted the intramolecular charge transfer in the system, leading to a hypsochromic shift in the fluorescence emission. The limit of detection was estimated to be 13.1 nM.[77]

4.2.2. Hypochlorite ions. Pyridine-thiophene-based fluorescent Probe 35 (Fig. 10) was prepared by Guo *et al.* for the recognition of hypochlorite ions. When excited at 380 nm, the probe displayed a bright cyan blue fluorescence emission, with a peak shoulder around 520 nm. Upon introducing hypochlorite ions, the emission peak started to quench and was completely quenched upon the addition of 2 equiv. of hypochlorite ions. This was attributed to the reaction of hypochlorite ions with the sulphur atom in the thiophene, which blocked the fluorophore that quenched the fluorescence emission of the probe. The detection limit was estimated to be 32 nM.[78] New thiophene-carbazole-based fluorescent Probe 36 (Fig. 10) was prepared by Feng *et al.* for the ratiometric analysis of hypochlorite ions in the solution state. When excited at 415 nm, the probe exhibited red fluorescence with an emission peak at 638 nm. Hypsochromic shift was observed upon introducing hypochlorite ions, with a new peak shoulder at 514 nm, revealing bright greenish blue fluorescence. This was ascribed to the reaction between the hypochlorite ions and the sulphur atom in the thiophene that restricted the intramolecular charge transfer in the system, leading to greenish blue fluorescence emission, and the limit of detection was found to be 10.8 nM.[56]

4.2.3. Halogen ions. New phenylquinazoline-thiophene-based fluorescent Probe 14 was designed by Harsha *et al.* for the recognition of iodine ions. When excited at 362 nm, the probe exhibited a strong blue fluorescence peak at 427 nm, but upon the addition of iodine ions, the fluorescence intensity peak at 427 nm decreased, and the fluorescence was completely quenched. This was ascribed to the chelation of iodine

with the probe that hindered the charge transfer in the probe, which blocked the fluorophore from emitting fluorescence, and the detection limit and quantification were estimated to be 0.17 μM and 0.52 μM, respectively.[59] Saini *et al.* synthesized the novel thiophene-hydrazone-based fluorescent Probe 16 for the detection of fluorine ions in the solution state. When excited at 365 nm, the probe exhibited enhanced green fluorescence with an intensity peak at 530 nm in THF. Upon the addition of fluorine ions, the peak at 530 nm decreased, and the fluorescence emission was completely quenched. This was ascribed to the chelation effect of fluorine ions with the probe that restricted the electron transfer in the system, which quenched the fluorescence emission of the probe, and the detection limit was found to be 18.95 nM.[61]

4.2.4. Sulfite ions. Pyrene-thiophene-derived fluorescent Probe 1 was prepared by Chao *et al.* and used for the estimation of bisulfite anions in an aqueous medium. Upon excitation at 366 nm, the probe revealed a peak at 530 nm by emitting yellow fluorescence. Upon introducing bisulfite ions to the probe, the emission peak at 530 nm gradually reduced, and a new emission band at 420 nm arose by producing blue fluorescence. This can be ascribed to the disruption of the electrophilic C=C bond in the π-conjugated system through the nucleophilic attack of bisulfite ions, hindering the charge transfer from donor base to acceptor base in the system, and the detection limit was found to be 0.77 μM.[38] Thiophene-pyrazoline-based fluorescent Probe 37 (Fig. 10) was prepared by Uchacz *et al.* for the selective recognition of sulphite anions in an aqueous medium. When excited at 407 nm, the probe exhibited a fluorescent emission peak at 462 nm with no significant fluorescent emission. On introducing sulphite ions, the new peak at 475 nm emerged with bright blue fluorescence intensity, which was ascribed to the disruption of the system by Michael addition reaction of the sulphite ion with the probe that restricted the intramolecular charge transfer in the system, which led to the blue fluorescent emission, and the limit of detection was estimated to be 4.87 μM.[79]

4.2.5. Pyrophosphate ions. Xing *et al.* prepared salicylic aldehyde-thiophene-based fluorescent Probe 7, which displayed a bright yellow fluorescence on complexation with indium ions. The fluorescence intensity peak at 550 nm decreased upon the addition of pyrophosphate ions, and complete quenching of fluorescence emission was noticed upon adding 10 equiv. of pyrophosphate ions. This was ascribed to the removal of indium ions from the complex by pyrophosphate ions, with more binding affinity to indium ions than to the probe, which led to the free existence of the probe, therefore causing the quenching effect, and the detection limit was evaluated to be 4.4 μM.[47] Symmetrical Schiff's base fluorescent Probe 10, prepared by Xing *et al.*, on complexation with gallium ions enabled a significant green fluorescence emission. On introducing pyrophosphate ions, the emission intensity peak at 513 nm of the complex decreased, which was ascribed to the higher binding affinity of pyrophosphate ions towards gallium ions, which promoted the free existence of the probe and initiated the electron transfer in the system, hindering the fluorescence emission.[50] Novel thiophene-rhodamine-based fluorescent Probe 30 was developed by Wang *et al.*, which, on chelation with ferric ions, exhibited a bright red fluorescence response, but on introducing pyrophosphate ions, the peak at 584 nm decreased gradually. This was due to the competitive binding affinity of pyrophosphate towards ferric ions that inhibited the structural change caused by ferric ion chelation in the probe, which quenched the fluorescence response.[74]

4.3. Sensing biological molecules

Complying with all thiophene-based probes used for sensing biological molecules is illustrated in Fig. 10.

4.3.1. Amino acids. Thiophene-based fluorescent Probe 8 designed by Sarkar *et al.* exhibited enhanced blue fluorescence on complexation with mercury ions. Upon the addition of cysteamine, an amino acid, to the probe complex, the emission peak, which was shouldered at 452 nm, was reduced, and the fluorescence intensity was completely quenched upon the addition of 8 μM of cysteamine. This fluorescence quenching was ascribed to the higher complexation affinity of mercury ions towards cysteamine than the probe. This led to the free existence of the probe without complexation, which quenched the fluorescence emission.[48] Thiophene-based polymer fluorescent Probe 31 was developed by Guo *et al.*, which, on complexation with copper ions, did not exhibit any significant fluorescence emission. Upon introducing homocysteine/glutathione, fluorescence enhancement was noticed due to the disruption of the coordination of the probe with copper ions, which allowed the probe to freely exist, reviving the fluorescent emission of the probe. The limit of detection was found to be 20 μM.[75] A. Kumar and P. S. Chae designed thiophene-benzimidazole-derived Probe 23 that has no significant fluorescent emission in coordination with mercury ions. Upon the addition of lysine, the solution revived its fluorescent emission. This was ascribed to the competitive binding ability of the lysine towards mercury ions, rather than the probe, which allowed the probe to exist freely in the solution, enhancing the fluorescent emission, and the detection limit was estimated to be 5 nM.[67]

4.3.2. Picric acid. New pyrene-thiophene-based fluorescent Probe 17 was synthesized by Kundu *et al.* for the selective detection of picric acid in an aqueous medium. When excited at 368 nm, the probe exhibited a fluorescence intensity peak shouldered at 425 nm with a strong blue fluorescence emission. However, upon the addition of picric acid, there was a bathochromic shift of about 37 nm with the fluorescence intensity quenching, and a new peak was shouldered at 462 nm. This can be attributed to the binding of picric acid with the probe that restricts C=N isomerization, which quenches fluorescence.[62] Lu *et al.* prepared thiophene aromatic amine-based fluorescent Probe 38 (Fig. 10) for the selective sensing of picric acid in both the solution and solid states. The probe exhibited a blue fluorescence emission with a peak at 454 nm. Upon introducing 1 eq. of picric acid to the probe solution, 30% of the fluorescence emission was quenched.

This was due to the protonation of the probe that hindered the charge transfer in the system, which quenched the fluorescence emission at 454 nm, and the limit of detection was found to be 5.7 μM.[80] D. Giri and S. K. Patra developed copolymer fluorescent Probe 39 (Fig. 10), which contained thiophene, carbazole, and fluorene groups functionalized in it, and was used for the selective recognition of picric acid in both solution and solid states. The probe exhibited a bright blue fluorescence emission, with a dual peak and a major peak contributing at 464 nm. Upon introducing picric acid into the solution, the emission peak at 464 nm started to decrease, indicating the quenching of the fluorescence emission. This was ascribed to the restricted electron transfer in the system that quenched the fluorescence emission, and the detection limit was estimated to be 0.9 μM.[81]

4.4. Bioimaging of live cells

The turn-on fluorescent response of Probe 11 upon complexation with Al^{3+} synthesized by Yin *et al.* was utilized for imaging Al^{3+} ions in live HeLa cells. Initially, the cells were incubated in 10 μM of Probe 11 for 60 min, which had no significant fluorescence response. However, upon additional incubation with 10 μM Al^{3+} solution for 30 min, a strong blue fluorescence was noticed in the blue channel owing to the complexation of Al^{3+} ions with Probe 11.[55] The turn-off fluorescence of Probe 35 prepared by Guo *et al.* was employed in imaging ClO^- ions in live MCF-7 cells. The cells were incubated with Probe 35, which emitted a bright green fluorescence response in the green channel, whereas in the pre-treated cells incubated in the ClO^- solution, when observed under a microscope at an excitation wavelength of 405 nm, no significant emission was noticed in the green channel, which was ascribed to the binding of ClO^- ions with the sulphur atom of the thiophene moiety in Probe 35.[78] To evaluate the practical utility of Probe 30 synthesized by Wang *et al.*, the estimation of Fe^{3+} ions in living cells was executed by incubating HeLa cells with Probe 30, which had no significant fluorescence emission. However, upon incubating the pre-treated cells in Fe^{3+} solution, a strong yellow emission was noticed in the yellow channel, which was due to the chelation of Fe^{3+} with Probe 30.[74] The turn-on fluorescent ability of Probe 27 was incorporated into the biological system for imaging Fe^{3+} ions in live cells. First, HepG2 cells were incubated with 10 μM of Probe 27, which had no considerable emission in the green channel. However, upon introducing the pre-treated cells in Fe^{3+} solution, a considerable amount of green fluorescence emission was noticed in the green channel, which was explained by the binding of Fe^{3+} ions with Probe 27.[71]

The hypsochromic shift of Probe 6 was engaged in imaging Hg^{2+} ions in live cells. Primarily, the DL cells were incubated in 10 μM of Probe 6 solution, in which a notable green fluorescence was observed. Further, upon incubating the cells with Hg^{2+} solution, a hypsochromic shift with blue-green fluorescence emission was observed. This was attributed to the complexation of the Hg^{2+} ions with Probe 6.[43] The enhanced fluorescence response of Probe 1 synthesized by Chao *et al.* was utilized in imaging HSO_3^- ions in living cells. Initially, the A549 cells were incubated with 10 μM Probe 1, which revealed a strong yellow fluorescence in the yellow channel but weak blue fluorescence in the blue channel. On further incubating the pre-treated cells with HSO_3^- solution, strong blue fluorescence was noticed in the blue channel due to the binding of the HSO_3^- ions with Probe 1.[38] The enhancement in fluorescence emission of Probe 26 synthesized by Musib *et al.* was employed in imaging Zn^{2+} ions in live cells. A549 cells were incubated in 20 μM of Probe 26, and weak cyan blue fluorescence emission was noted. Upon additional incubation with Zn^{2+} solution, enhanced cyan blue fluorescence emission was noticed due to the chelation of Zn^{2+} with Probe 26.[70] The turn-on fluorescence response of Probe 25 was utilized in imaging Zn^{2+} in living cells. Initially, the HeLa cells were incubated with 30 μM of Probe 25 for 20 min, where no notable emission was recorded in the green channel. Upon incubating the pre-treated cells in Zn^{2+} solution, a strong green fluorescence emission was noticed, which was ascribed to the complexation of Zn^{2+} ions with Probe 25.[69] To evaluate the potential of Probe 52 in the bioimaging of Fe^{3+} ions, HepG2 cells were incubated with 50 μM Probe 52 for 2 h, which had no considerable fluorescence emission in the red channel. However, treating the pre-treated cells with Fe^{3+} ions showed a strong red fluorescence emission in the red channel owing to its chelation of Fe^{3+} ions towards Probe 52.[92] The turn-off fluorescence of Probe 44 prepared by Musikavanhu *et al.* was employed in imaging Hg^{2+} ions. The HeLa cells were incubated in 10 μM of Probe 44, which showed a bright cyan blue fluorescence emission in the blue channel. When the pre-treated cells were incubated in Hg^{2+} solution, the fluorescence emission was quenched, and no significant fluorescence emission was recorded, which was ascribed to the binding of Hg^{2+} ions with Probe 44.[85] The turn-on fluorescence response of Probe 46 was employed in imaging Hg^{2+} ions in live cells. MCF-7 cells were incubated in 10–70 μM of Probe 46 and Probe 46+ Hg^{2+} ion complexes. The cells incubated in Probe 46 had no considerable fluorescence emission in the red channel, whereas the cells incubated in Probe 46+ Hg^{2+} ion complex revealed a strong red fluorescence emission in the red channel. This was due to the chelation of Hg^{2+} ions with Probe 46.[87]

To elucidate the biological application of Probe 19, imaging Zn^{2+}/Al^{3+} ions was demonstrated in live cells. HeLa cells were incubated in 10 my M of Probe 19 for 30 min, which revealed no obvious fluorescence emission. Upon further incubation with Zn^{2+}/Al^{3+} solution for 60 min, a strong green and blue fluorescence emission was observed in blue and green channels, respectively. This was ascribed to the chelation of Zn^{2+}/Al^{3+} ions with Probe 19.[64] To examine the turn-on fluorescent response of Probe 51, bioimaging of Fe^{3+}/Al^{3+} ions in live cells was performed. The HeLa cells were incubated in Probe 51 solution, which revealed no significant fluorescence emission. However, upon incubating the pre-treated cells in 100 μM of Fe^{3+}/Al^{3+} solution, a bright yellow fluorescence was noticed, which was due to the complexation of these ions with Probe

51.[53] The bathochromic shift of Probe 36 upon the addition of ClO^- ions was utilized for imaging ClO^- ions in live cells. HEK293 cells were incubated in 10 μM of Probe 36, which exhibited a bright red fluorescence emission in the cytoplasm at the red channel. Then, when it was incubated in 45 μM of ClO^- solution, a bright green fluorescence emission was noticed in the green channel, which can be attributed to the recognition of ClO^- by the sulphur atoms in the thiophene ring of Probe 36.[56] Zhao *et al.* synthesized Probe 4 for imaging CN^- ions in live cells. The cells were treated with 10 μM of Probe 4 for 30 min, which exhibited a feeble red fluorescence response in the red channel, whereas upon incubating the pre-treated cells with CN^- ions, a bright red fluorescence response was observed, which can be attributed to the disruption of the charge transfer in Probe 4 by CN^- ions.[41]

5. Conclusions

Conclusively, thiophene rings have proven their versatility over decades by portraying them in multiple roles, such as an electron donor, a recognition moiety, and a fluorophore, when incorporated into the construction of fluorescent probes based on ICT and PET mechanisms. This has aided in overcoming the traditional complications of low sensitivity and poor selectivity towards sensing biological and chemical analytes. The specificity and selectivity towards analytes are due to the presence of a sulphur atom in the ring, which contributes to the higher electron charge density than other heterocyclic compounds. Additionally, the good charge mobility and high photophysical tunability of thiophenes have proven them to be an excellent alternative for sensing analytes. However, the high polarizability of the sulphur atom in the ring results in conjugating chain stability, which complements the stability of molecules in biological systems. This allows the sensor with a thiophene substituent to accurately and specifically detect analytes in biological systems while offering a broad range of photophysical tunability.

6. Future prospects

Looking ahead, thiophene-based probes hold immense potential for expansion into advanced biomedical applications beyond conventional fluorescence sensing, particularly in areas like photoacoustic imaging (PAI)[98] and photodynamic therapy (PDT).[99] Their strong NIR absorption, excellent photothermal conversion efficiency, and ability to generate reactive oxygen species (ROS) make them highly suitable for non-invasive imaging and targeted therapeutic approaches.[100] The inherent advantages of thiophene derivatives—such as high photostability, tunable electronic properties, strong charge mobility, and sulfur-induced selectivity—make them ideal candidates for developing smart, responsive probes. However, limitations such as poor water solubility, potential photobleaching, and limited deep-tissue penetration remain major challenges. Addressing these issues through rational molecular design and hybrid systems, such as conjugation with biocompatible polymers or nanomaterials, can improve bioavailability and functionality. Additionally, structure–activity relationship (SAR) studies, development of dual-mode theranostic agents, and incorporation of stimuli-responsive elements (*e.g.*, pH, redox, and enzymes) offer promising routes to enhance selectivity, therapeutic efficacy, and controlled activation. Continued exploration of dual-mode theranostic agents combining imaging and therapy is also a key avenue. Addressing these challenges through targeted synthetic innovation and mechanistic insight will position thiophene-based systems as powerful multifunctional platforms for precision diagnostics and therapy.

Author contributions

Aakash Venkatesan: conceptualization, formal analysis, investigation and writing – original draft. Anila Rose Cherian: investigation, validation and writing – review & editing. Aatika Nizam: supervision, conceptualization, validation and writing – review & editing.

Conflicts of interest

There are no conflicts to declare.

Data availability

This review article does not contain any original data. All data analyzed and discussed in this manuscript are publicly available in the cited references.

Acknowledgements

I would like to thank Christ University for their constant encouragement and support.

References

1 S. Cárdenas and M. Valcárcel, *TrAC, Trends Anal. Chem.*, 2005, **24**, 477–487, DOI: 10.1016/j.trac.2005.03.006.
2 A. P. V. S, P. Joseph, K. D. S. C. G, S. Lakshmanan, T. Kinoshita and S. Muthusamy, *Mater. Sci. Eng., C*, 2017, **78**, 1231–1245, DOI: 10.1016/j.msec.2017.05.018.
3 D. Grieshaber, R. MacKenzie, J. Vörös and E. Reimhult, *Sensors*, 2008, **8**, 1400–1458, DOI: 10.3390/s80314000.
4 M. G. Gioia, P. Andreatta, S. Boschetti and R. Gatti, *J. Pharm. Biomed. Anal.*, 2008, **48**, 331–339, DOI: 10.1016/j.jpba.2008.01.026.
5 J. Fan, C. Ye, S. Feng, G. Zhang and J. Wang, *Talanta*, 1999, **50**, 893–898, DOI: 10.1016/S0039-9140(99)00183-6.

6 M. Liu, Z. Lin and J. M. Lin, *Anal. Chim. Acta*, 2010, **670**, 1–10, DOI: 10.1016/j.aca.2010.04.039.
7 T. Wu, Y. Guan and J. Ye, *Food Chem.*, 2007, **100**, 1573–1579, DOI: 10.1016/j.foodchem.2005.12.042.
8 C. Lino, S. Barrias, R. Chaves, F. Adega, P. Martins-Lopes and J. R. Fernandes, *Biochim. Biophys. Acta, Rev. Cancer*, 2022, **1877**, 188726, DOI: 10.1016/j.bbcan.2022.188726.
9 Y. H. Shin, M. T. Gutierrez-Wing and J. W. Choi, *J. Electrochem. Soc.*, 2021, **168**, 017502, DOI: 10.1149/1945-7111/abd494.
10 M. Arshad, J. R. A. T, V. Joseph and A. Joseph, *J. Lumin.*, 2023, **258**, 119818, DOI: 10.1016/j.jlumin.2023.119818.
11 Y. Yang, H. Wang, K. Su, Y. Long, Z. Peng, N. Li and F. Liu, *J. Mater. Chem.*, 2011, **21**, 11895, DOI: 10.1039/c0jm04444j.
12 T. Oh, J. H. Sung, D. A. Tatosian, M. L. Shuler and D. Kim, *Cytometry, Part A*, 2007, **71**, 857–865, DOI: 10.1002/cyto.a.20427.
13 H. Feng, Z. Zhang, Q. Meng, H. Jia, Y. Wang and R. Zhang, *Adv. Sci.*, 2018, **5**, 1800397, DOI: 10.1002/advs.201800397.
14 A. Afrin, A. Jayaraj and M. S. Gayathri, *Sens. Diagn.*, 2023, **2**, 988–1076, DOI: 10.1039/D3SD00110E.
15 F. Joy, A. V, J. Devasia and A. Nizam, *Appl. Spectrosc. Rev.*, 2023, 1–30, DOI: 10.1080/05704928.2023.2276925.
16 Y. Tian, X. Huang, H. Li, Q. Chen, X. Gong, H. Chen, M. Fan and Z. Gong, *Anal. Chim. Acta*, 2024, **1285**, 342009, DOI: 10.1016/j.aca.2023.342009.
17 N. I. Georgiev, V. V. Bakov and V. B. Bojinov, *Photonics*, 2022, **9**, 994, DOI: 10.3390/photonics9120994.
18 T. Li, H. Pang, Q. Wu, M. Huang, J. Xu, L. Zheng, B. Wang and Y. Qiao, *Int. J. Mol. Sci.*, 2022, **23**, 6259, DOI: 10.3390/ijms23116259.
19 R. Wang, X. Gu, Q. Li, J. Gao, B. Shi, G. Xu, T. Zhu, H. Tian and C. Zhao, *J. Am. Chem. Soc.*, 2020, **142**, 15084–15090, DOI: 10.1021/jacs.0c06533.
20 L. Wu, C. Huang, B. P. Emery, A. C. Sedgwick, S. D. Bull, X. P. He, H. Tian, J. Yoon, J. L. Sessler and T. D. James, *Chem. Soc. Rev.*, 2020, **49**, 5110–5139, DOI: 10.1039/C9CS00318E.
21 D. Udhayakumari, *J. Fluoresc.*, 2024, 1–30, DOI: 10.1007/s10895-024-03843-1.
22 Z. Y. Li, X. L. Cui, M. M. Xiao, J. Y. Miao, B. X. Zhao and Z. M. Lin, *Dyes Pigm.*, 2021, **193**, 109481, DOI: 10.1016/j.dyepig.2021.109481.
23 X. Meng, L. You, S. Li, Q. Sun, X. Luo, H. He, J. Wang and F. Zhao, *RSC Adv.*, 2020, **10**, 37735–37742, DOI: 10.1039/D0RA07330J.
24 R. J. Abdel-Jalil, A. R. Ibrahim and O. K. Abou-Zied, *Chem. Phys. Lett.*, 2023, **813**, 140299, DOI: 10.1016/j.cplett.2023.140299.
25 S. D. Padghan, L. C. Wang, W. C. Lin, J. W. Hu, W. C. Liu and K. Y. Chen, *ACS Omega*, 2021, **6**, 5287–5296, DOI: 10.1021/acsomega.0c05409.
26 H. Y. Tsai and K. Y. Chen, *J. Lumin.*, 2014, **149**, 103–111, DOI: 10.1016/j.jlumin.2014.01.031.
27 R. L. Camacho-Mendoza, E. Aquino-Torres, J. Cruz-Borbolla, J. G. Alvarado-Rodríguez, O. Olvera-Neria, J. Narayanan and T. Pandiyan, *Struct. Chem.*, 2014, **25**, 115–126, DOI: 10.1007/s11224-013-0254-9.
28 X. Cheng, S. Li, H. Jia, A. Zhong, C. Zhong, J. Feng, J. Qin and Z. Li, *Chem. – Eur. J.*, 2012, **18**, 1691–1699, DOI: 10.1002/chem.201102376.
29 R. S. Fernandes, N. S. Shetty, P. Mahesha and S. L. Gaonkar, *J. Fluoresc.*, 2022, 1–38, DOI: 10.1007/s10895-021-02833-x.
30 S. C. Rasmussen, S. J. Evenson and C. B. McCausland, *Chem. Commun.*, 2015, **51**, 4528–4543, DOI: 10.1039/C4CC09206F.
31 I. F. Perepichka, D. F. Perepichka and H. Meng, *Handbook of Thiophene-Based Materials: Applications in Organic Electronics and Photonics*, John Wiley & Sons, Hoboken, NJ, 2009, p. 2. DOI: 10.1002/9780470745533.ch19.
32 A. C. Grimsdale, K. L. Chan, R. E. Martin, P. G. Jokisz and A. B. Holmes, *Chem. Rev.*, 2009, **109**, 897–1091, DOI: 10.1021/cr000013v.
33 I. F. Perepichka, D. F. Perepichka, H. Meng and F. Wudl, *Adv. Mater.*, 2005, **17**, 2281–2305, DOI: 10.1002/adma.200500461.
34 H. A. Z. Sabek, A. M. M. Alazaly, D. Salah, H. S. Abdel-Samad, M. A. Ismail and A. A. Abdel-Shafi, *RSC Adv.*, 2020, **10**, 43459–43471, DOI: 10.1039/D0RA08433F.
35 S. Jaswal and J. Kumar, *Mater. Today: Proc.*, 2020, **26**, 566–580, DOI: 10.1016/j.matpr.2019.12.161.
36 M. HeeáLee and J. SeungáKim, *Chem. Soc. Rev.*, 2015, **44**, 4185–4191, DOI: 10.1039/C4CS00280F.
37 F. Bureš, *RSC Adv.*, 2014, **4**, 58826–58851, DOI: 10.1039/C4RA11264D.
38 J. Chao, X. Wang, Y. Liu, Y. Zhang, F. Huo, C. Yin, M. Zhao, J. Sun and M. Xu, *Sens. Actuators, B*, 2018, **272**, 195–202, DOI: 10.1016/j.snb.2018.05.058.
39 N. Bhuvanesh, S. Suresh, P.R Kumar, E.M Mothi, K. Kannan, V. R. Kannan and R. Nandhakumar, *J. Photochem. Photobiol., A*, 2018, **360**, 6–12, DOI: 10.1016/j.jphotochem.2018.04.027.
40 P. Purushothaman and S. Karpagam, *ACS Omega*, 2022, **7**, 41361–41369, DOI: 10.1021/acsomega.2c05157.
41 Y. Zhao, L. Feng, X. Meng and J. Guan, *Dyes Pigm.*, 2020, **183**, 108713, DOI: 10.1016/j.dyepig.2020.108713.
42 M. Chemchem, I. Yahaya, B. Aydıner, N. Seferoğlu, O. Doluca, N. Merabet and Z. Seferoğlu, *Tetrahedron*, 2018, **74**, 6897–6906, DOI: 10.1016/j.tet.2018.10.008.
43 S. S. Razi, R. Ali, R. C. Gupta, S. K. Dwivedi, G. Sharma, B. Koch and A. Misra, *J. Photochem. Photobiol., A*, 2016, **324**, 106–116, DOI: 10.1016/j.jphotochem.2016.03.015.
44 H. Niu, J. Liu, H. M. O'Connor, T. Gunnlaugsson, T. D. James and H. Zhang, *Chem. Soc. Rev.*, 2023, **52**, 2322–2357, DOI: 10.1039/D1CS01097B.
45 G. T. Selvan, C. Varadaraju, R. T. Selvan, I. V. M. V. Enoch and P. M. Selvakumar, *ACS Omega*, 2018, **3**, 7985–7992, DOI: 10.1021/acsomega.8b00748.

46 N. Boens, V. Leen and W. Dehaen, *Chem. Soc. Rev.*, 2012, **41**, 1130–1172, DOI: 10.1039/C1CS15132K.
47 Y. Xing, Z. Liu, Y. Xu, H. Wang, L. Li, B. Li, X. Yang, M. Pei and G. Zhang, *New J. Chem.*, 2020, **44**, 13875–13881, DOI: 10.1039/D0NJ03076G.
48 S. Sarkar, S. Roy, R. N. Saha and S. S. Panja, *J. Fluoresc.*, 2018, **28**, 427–437, DOI: 10.1007/s10895-017-2204-1.
49 E. Karakuş, *Turk. J. Chem.*, 2020, **44**, 941–949, DOI: 10.3906/kim-2003-41.
50 Y. Xing, Z. Liu, B. Li, L. Li, X. Yang and G. Zhang, *Sens. Actuators, B*, 2021, **347**, 130497, DOI: 10.1016/j.snb.2021.130497.
51 P. Yin, Q. Niu, T. Wei, T. Li, Y. Li and Q. Yang, *J. Photochem. Photobiol., A*, 2020, **389**, 112249, DOI: 10.1016/j.jphotochem.2019.112249.
52 F. Kolcu, D. Erdener and İ. Kaya, *Inorg. Chim. Acta*, 2020, **509**, 119676, DOI: 10.1016/j.ica.2020.119676.
53 K. P. Wang, J. P. Chen, S. J. Zhang, Y. Lei, H. Zhong, S. Chen, X. H. Zhou and Z. Q. Hu, *Anal. Bioanal. Chem.*, 2020, **409**, 5547–5554, DOI: 10.1007/s00216-017-0490-8.
54 M. Li, X. Zhang, Y. Fan and C. Bi, *Luminescence*, 2016, **31**, 851–855, DOI: 10.1002/bio.3041.
55 M. Rangasamy and K. Palaninathan, *Inorg. Chem. Commun.*, 2019, **101**, 177–183, DOI: 10.1016/j.inoche.2019.01.038.
56 A. Feng, P. Liu, Q. Liang, X. Zhang, L. Huang, Y. Jia, M. Xie, Q. Yan, C. Li and S. Wang, *Dyes Pigm.*, 2020, **180**, 108492, DOI: 10.1016/j.dyepig.2020.108492.
57 K. Mahesh and S. Karpagam, *Sens. Actuators, B*, 2017, **251**, 9–20, DOI: 10.1016/j.snb.2017.05.014.
58 S. Rajappa and V. K. Gumaste, *Adv. Heterocycl. Chem.*, 2013, **108**, 1–161, DOI: 10.1016/B978-0-12-404598-9.00001-8.
59 K. G. Harsha, B. A. Rao, T. R. Baggi, S. Prabhakar and V. J. Rao, *Photochem. Photobiol. Sci.*, 2020, **19**, 1707–1716, DOI: 10.1039/D0PP00193G.
60 H. H. Hammud, S. El Shazly, G. Sonji, N. Sonji and K. H. Bouhadir, *Spectrochim. Acta, Part A*, 2015, **150**, 94–103, DOI: 10.1016/j.saa.2015.05.038.
61 N. Saini, C. Wannasiri, S. Chanmungkalakul, N. Prigyai, V. Ervithayasuporn and S. Kiatkamjornwong, *J. Photochem. Photobiol., A*, 2019, **385**, 112038, DOI: 10.1016/j.jphotochem.2019.112038.
62 B. K. Kundu, S. M. Mobin and S. Mukhopadhyay, *New J. Chem.*, 2019, **43**, 11483–11492, DOI: 10.1039/C9NJ02342A.
63 M. M. Mathew and A. Sreekanth, *Inorg. Chim. Acta*, 2021, **516**, 120149, DOI: 10.1016/j.ica.2020.120149.
64 Y. Li, Q. Niu, T. Wei and T. Li, *Anal. Chim. Acta*, 2019, **1049**, 196–212, DOI: 10.1016/j.aca.2018.10.043.
65 K. Tiwari, M. Mishra and V. P. Singh, *RSC Adv.*, 2013, **3**, 12124–12132, DOI: 10.1039/C3RA41573B.
66 V. Govindasamy, S. Perumal, I. Sekar, B. Madheswaran, S. Karuppannan and S. B. Kuppannan, *J. Fluoresc.*, 2021, **31**, 667–674, DOI: 10.1007/s10895-021-02690-8.
67 A. Kumar and P. S. Chae, *Sens. Actuators, B*, 2019, **281**, 933–944, DOI: 10.1016/j.snb.2018.11.023.
68 L. Feng, Y. Deng, X. Wang and M. Liu, *Sens. Actuators, B*, 2017, **245**, 441–447, DOI: 10.1016/j.snb.2017.01.184.
69 M. S. Kim, D. Yun, J. B. Chae, H. So, H. Lee, K. T. Kim, M. Kim, M. H. Lim and C. Kim, *Sensors*, 2019, **19**, 5458, DOI: 10.3390/s19245458.
70 D. Musib, L. R. Devi, M. K. Raza, S. B. Chanu and M. Roy, *Chem. Lett.*, 2020, **49**, 473–476, DOI: 10.1246/cl.200001.
71 B. Lim, B. Baek, K. Jang, N. K. Lee, J. H. Lee, Y. Lee, J. Kim, J. Park, S. Kim, N. W. Kang, S. Hong, D. D. Kim, I. Kim, H. Hwang and J. Lee, *Dyes Pigm.*, 2019, **169**, 51–59, DOI: 10.1016/j.dyepig.2019.05.008.
72 A. L. Berhanu, S. Bhogal, I. Mohiuddin, A. Grover, A. K. Malik and J. S. Aulakh, *J. Fluoresc.*, 2022, **32**, 1247–1259, DOI: 10.1007/s10895-022-02914-5.
73 M. Üçüncü, *J. Fluoresc.*, 2023, **33**, 707–712, DOI: 10.1007/s10895-022-03117-8.
74 K. P. Wang, W. J. Zheng, Y. Lei, S. J. Zhang, Q. Zhang, S. Chen and Z. Q. Hu, *J. Lumin.*, 2019, **208**, 468–474, DOI: 10.1016/j.jlumin.2019.01.017.
75 C. Guo, P. Li, M. Pei and G. Zhang, *Sens. Actuators, B*, 2015, **221**, 1223–1228, DOI: 10.1016/j.snb.2015.07.105.
76 H. Cho, J. B. Chae and C. Kim, *Inorg. Chem. Commun.*, 2018, **97**, 171–175, DOI: 10.1016/j.inoche.2018.09.037.
77 A. Popczyk, Y. Cheret, A. El-Ghayoury, B. Sahraoui and J. Mysliwiec, *Dyes Pigm.*, 2020, **177**, 108300, DOI: 10.1016/j.dyepig.2020.108300.
78 H. Guo, J. Lin, L. Zheng and F. Yang, *Spectrochim. Acta, Part A*, 2021, **256**, 119744, DOI: 10.1016/j.saa.2021.119744.
79 T. Uchacz, G. Jajko, A. Danel, P. Szlachcic and S. Zapotoczny, *New J. Chem.*, 2019, **43**, 874–883, DOI: 10.1039/C8NJ05017A.
80 X. Lu, G. Zhang, D. Li, X. Tian, W. Ma, S. Li, Q. Zhang, H. Zhou, J. Wu and Y. Tian, *Dyes Pigm.*, 2019, **170**, 107641, DOI: 10.1016/j.dyepig.2019.107641.
81 D. Giri and S. K. Patra, *J. Mater. Chem. C*, 2020, **41**, 14469–14480, DOI: 10.1039/D0TC03310C.
82 H. Wang, P. Wang, L. Niu, C. Liu, Y. Xiao, Y. Tang and Y. Chen, *Spectrochim. Acta, Part A*, 2022, **278**, 121257, DOI: 10.1016/j.saa.2022.121257.
83 G. A. Zalmi, D. N. Nadimetla, A. L. Puyad, K. U. Narvekar, R. V. Hangarge and S. V. Bhosale, *ChemistrySelect*, 2024, **9**, e202303559, DOI: 10.1002/slct.202303559.
84 N. Thakur, P. Kandwal and R. Pandey, *Ind. Eng. Chem. Res.*, 2023, **62**, 12864–12879, DOI: 10.1021/acs.iecr.3c01806.
85 B. Musikavanhu, S. Muthusamy, D. Zhu, Z. Xue, Q. Yu, C. N. Chiyumba, J. Mack, T. Nyokong, S. Wang and L. Zhao, *Spectrochim. Acta, Part A*, 2022, **264**, 120338, DOI: 10.1016/j.saa.2021.120338.
86 Z. Yang, S. Chen, Y. Zhao, P. Zhou and Z. Cheng, *Sens. Actuators, B*, 2018, **266**, 422–428, DOI: 10.1016/j.snb.2018.03.148.
87 B. Li, F. Tian and Y. Hua, *RSC Adv.*, 2022, **12**, 21129–21134, DOI: 10.1039/D2RA02185D.
88 P. Purushothaman and S. Karpagam, *Spectrochim. Acta, Part A*, 2024, **305**, 123518, DOI: 10.1016/j.saa.2023.123518.

89 H. Kim, M. Lee, J. J. Lee, E. K. Min, K. T. Kim and C. Kim, *J. Photochem. Photobiol., A*, 2022, **428**, 113882, DOI: 10.1016/j.jphotochem.2022.113882.
90 J. Isaad, F. Malek and A. El Achari, *J. Mol. Struct.*, 2022, **1270**, 133838, DOI: 10.1016/j.molstruc.2022.133838.
91 S. Roy, T. Mondal, D. Dey, M. V. Mane and S. S. Panja, *ChemistrySelect*, 2021, **6**, 10464–10479, DOI: 10.1002/slct.202102692.
92 Y. Liu, C. Zhao, X. Zhao, H. Liu, Y. Wang, Y. Du and D. Wei, *J. Environ. Sci.*, 2020, **90**, 180–188, DOI: 10.1016/j.jes.2019.12.005.
93 L. Naik, C. V. Maridevarmath, M. S. Thippeswamy, H. M. Savanur, I. A. M. Khazi and G. H. Malimath, *Mater. Chem. Phys.*, 2021, **260**, 124063, DOI: 10.1016/j.matchemphys.2020.124063.
94 X. Sun, J. Wang, Z. Shang, H. Wang, Y. Wang and S. Shuang, *J. Mol. Liq.*, 2024, **402**, 124788, DOI: 10.1016/j.molliq.2024.124788.
95 Y. Tao, Y. Jin, Y. Cui, T. Yu, J. Ji, W. Zhu, M. Fang and C. Li, *Spectrochim. Acta, Part A*, 2024, **310**, 123912, DOI: 10.1016/j.saa.2024.123912.
96 Z. Liu, Z. Yang, S. Chen, Y. Liu, L. Sheng, Z. Tian, D. Huang and H. Xu, *Microchem. J.*, 2020, **156**, 104809, DOI: 10.1016/j.microc.2020.104809.
97 B. Rani, A. Agarwala, D. Behera, V. P. Verma, A. P. Singh and R. Shrivastava, *Dyes Pigm.*, 2021, **194**, 109596, DOI: 10.1016/j.dyepig.2021.109596.
98 C. Li, C. Liu, Y. Fan, X. Ma, Y. Zhan, X. Lu and Y. Sun, *RSC Chem. Biol.*, 2021, **2**, 743–758, DOI: 10.1039/D0CB00225A.
99 E. Pang, R. Huang, S. Zhao, K. Yang, B. Li, Q. Tan, S. Tan, M. Lan, B. Wang and X. Song, *J. Mater. Chem. B*, 2022, **10**, 9848–9854, DOI: 10.1039/D2TB01772E.
100 Q. Liu, J. Tian, Y. Tian, Q. Sun, D. Sun, D. Liu, F. Wang, H. Xu, G. Ying, J. Wang and A. K. Yetisen, *Acta Biomater.*, 2021, **127**, 287–297, DOI: 10.1016/j.actbio.2021.03.064.